Journal of Hazardous Materials 274 (2014) 212–220

Contents lists available at ScienceDirect

Journal of Hazardous Materials

journal homepage: www.elsevier.com/locate/jhazmat

# Oxidative regeneration of toluene-saturated natural zeolite by gaseous ozone: The influence of zeolite chemical surface characteristics

Serguei Alejandro[a,b], Héctor Valdés[a,*], Marie-Hélène Manéro[d,e], Claudio A. Zaror[c]

[a] Laboratorio de Tecnologías Limpias (F. Ingeniería), Universidad Católica de la Santísima Concepción, Alonso de Ribera 2850, Concepción, Chile
[b] Núcleo de Energías Renovables (F. Ingeniería), Universidad Católica de Temuco, Rudecindo Ortega 02950, Temuco, Chile
[c] Departamento de Ingeniería Química (F. Ingeniería), Universidad de Concepción, Concepción, Correo 3, Casilla 160–C, Chile
[d] Université de Toulouse; INPT, UPS; Laboratoire de Génie Chimique, 4, Allée Emile Monso, F–31030 Toulouse, France
[e] CNRS; Laboratoire de Génie Chimique; F–31030 Toulouse, France

## HIGHLIGHTS

- Surface acidity of modified natural zeolite is related to its chemical reactivity.
- Brønsted acid sites are associated to toluene adsorption.
- Lewis acid sites could decompose ozone generating surface active oxygen species.
- Infrared spectra evidence active atomic oxygen and oxidation by-product formation.
- 2NH4Z1 sample shows the highest reactivity toward adsorbed toluene.

## ARTICLE INFO

*Article history:*
Received 2 December 2013
Received in revised form 1 April 2014
Accepted 2 April 2014
Available online 13 April 2014

*Keywords:*
Brønsted acid sites
Lewis acid sites
Ozone
Toluene
Zeolite

## ABSTRACT

In this study, the effect of zeolite chemical surface characteristics on the oxidative regeneration of toluene saturated-zeolite samples is investigated. A Chilean natural zeolite (53% clinoptilolite, 40% mordenite and 7% quartz) was chemically modified by acid treatment with hydrochloric acid and by ion-exchange with ammonium sulphate. Thermal pre-treatments at 623 and 823 K were applied and six zeolite samples with different chemical surface characteristics were generated. Chemical modification of natural zeolite followed by thermal out-gassing allows distinguishing the role of acidic surface sites on the regeneration of exhausted zeolites. An increase in Brønsted acid sites on zeolite surface is observed as a result of ammonium-exchange treatment followed by thermal treatment at 623 K, thus increasing the adsorption capacity toward toluene. High ozone consumption could be associated to a high content of Lewis acid sites, since these could decompose ozone into atomic active oxygen species. Then, surface oxidation reactions could take part among adsorbed toluene at Brønsted acid sites and surface atomic oxygen species, reducing the amount of adsorbed toluene after the regenerative oxidation with ozone. Experimental results show that the presence of adsorbed oxidation by-products has a negative impact on the recovery of zeolite adsorption capacity.



## 1. Introduction

Hazardous air pollutants such as volatile organic compounds (VOCs) are typically generated in chemical industries, posing a high risk to human health [1]. Industrial atmospheric emissions have been traditionally controlled using adsorption processes [2,3]. Once adsorbents are exhausted they need to be disposed or regenerated. Regeneration techniques such as chemical or thermal desorption are normally used by the industry, allowing valuable adsorbate recovery [4]. However, when recovery is not possible, further treatments are needed in order to eliminate adsorbed contaminants [5].

Recently, advanced oxidation processes, such as gas phase catalytic ozonation, have been proposed as an effective alternative to regenerate spent adsorbents [6,7]. Adsorption of toluene on synthetic zeolites (FauY, SilZ and ZSM-5) followed by ozonation, has

* Corresponding author. Tel.: +56 41 2345044; fax: +56 41 2345300.
*E-mail address:* hvaldes@ucsc.cl (H. Valdés).

http://dx.doi.org/10.1016/j.jhazmat.2014.04.006
0304-3894/

been proposed as a reliable process to oxidise adsorbed toluene on zeolite surface, resulting in a high degree of recovery on adsorption capacity [8–10]. However, there is a lack of information related to the effect of chemical surface characteristics of zeolites in these coupled processes. Separated processes for VOCs and gaseous ozone removal from industrial waste gas streams using synthetic and natural zeolites have been applied [11–16].

On one hand, Brønsted and Lewis acid sites have been claimed as responsible of VOCs removal by adsorption onto natural zeolites [11,12]. It has been indicated that weak base aromatic VOC molecules such as benzene, toluene and *p*-xylene could be adsorbed by a surface mechanism that includes interaction with Brønsted acid sites in the form of proton-donating hydroxyl groups of natural mordenite surface, forming hydrogen bonds; and with Lewis acid sites, generating a Lewis acid–base adduct [12]. On the other hand, weak and strong Lewis acid sites of natural and synthetic zeolites have been identified as the main active sites responsible of gaseous ozone removal [13–16]. Molecular ozone could be adsorbed *via* coordinative bonding at weak Lewis acid sites. Moreover, ozone could transform immediately after adsorption on strong Lewis acid sites and decomposes into $O_2$ and an active atom of oxygen that could participate in catalytic removal of ozone [15,16].

Unfortunately, the influence of chemical surface properties of natural and synthetic zeolites on VOC removal, using a sequential adsorption-ozonation treatment, at room temperature has not been fully studied yet. In this work, a Chilean natural zeolite is used as starting material; and it is chemically and thermally modified in order to generate a zeolite surface reach in a high content of Brønsted acid sites (using ammonium ion-exchange followed by thermal treatment at 623 K) or Lewis acid sites (using ammonium ion-exchange followed by thermal treatment at 823 K). The nature and strength of acidic surface sites resulting from the applied modification treatments are characterised by Fourier transform infrared (FTIR) spectroscopy using pyridine as a probe molecule. Toluene is chosen here as a target VOCs, since it represents a serious threat to human health [17]. Additionally, FTIR spectroscopy is employed to clarify the surface reaction mechanism that takes place between toluene and ozone on zeolite samples. Finally, zeolite surface active centres are identified and the natures of their interaction toward toluene and ozone are characterised at a molecular level.

## 2. Materials and methods

### 2.1. Materials

Chilean natural zeolite (53% clinoptilolite, 40% mordenite and 7% quartz) was provided by Minera Formas. Zeolite sample was ground and sieved to 0.3–0.425 mm; then was rinsed with ultra pure water, oven-dried at 398 K for 24 h, and stored in a desiccator until further use. Natural zeolite was modified by acid treatment using HCl (2.4 mol $dm^{-3}$), and by ion-exchange using ammonium sulphate (0.1 mol $dm^{-3}$), as reported elsewhere [14]. Acid-treated zeolite and ion exchanged zeolite were named ZH2.4 and NH4Z1, respectively. A second ion-exchange treatment was conducted to the NH4Z1 sample and a new zeolite sample with different chemical surface properties was obtained (2NH4Z1), as described in previous work [14]. Zeolite samples were thermally out-gassed in an oven at 623 K or 823 K (heating rate 10 K $min^{-1}$) during two hours prior to adsorption-ozonation experiments.

Toluene (99.8% purity) was provided by MERCK. Ozone was produced *in situ*, from synthetic dry air, using a Traigalaz 5LO ozone generator. The inlet concentration of ozone was fixed at 24.3 g $dm^{-3}$ in all experiments.

### 2.2. Physical–chemical characterisation of zeolite samples

Surface area of zeolite samples were obtained by nitrogen adsorption at 77 K, after zeolite out-gassing overnight at 623 K and 823 K, under vacuum [14]. Bulk chemical composition of natural and modified zeolite samples was obtained by X-ray fluorescence (XRF) using a RIGAKU Model 3072 spectrometer [18]. Density measurements of zeolite samples were carried out in an AccuPyc 1330 pycnometer using helium (99.995% purity) and registering the helium pressure change in a calibrated chamber [19]. Physical and chemical surface characteristics of natural and modified zeolite samples are listed in Table 1. Surface areas ($S$) were calculated by applying the Langmuir adsorption model to nitrogen adsorption data. After acid treatment of natural zeolite, the surface area and the Si/Al ratio increase for ZH2.4, as a consequence of a de-cationisation and de-alumination mechanisms [20]. The high value of ZH2.4 surface area could be related to an enhancement on zeolite microporosity. During the de-alumination process, the exchange of hydrated cations by $H^+$ could have risen micropore accessibility, eventually blocked before the acid treatment [20]. Pore opening expansion could result also from a de-cationisation process, generating the so-called "open structures" that could lead to a decrease in diffusion resistance inside the zeolite framework [14]. Additionally, surface areas of NZ and ZH2.4 samples decrease after thermal treatment at 823 K. This could be related to the interaction of compensating cations and water in the zeolite framework. During the out-gassing process at 823 K, water molecules leave the zeolite, destabilising the zeolite charge structure. In order to correct this, it has been suggested that compensating cations in the zeolite framework, form bonds with network oxygen atoms, affecting the zeolite structure channels [15]. However, in the ammonium-exchanged zeolites, surface areas are increased after thermal treatment at 823 K. Such increase in the value of surface areas could be related to the elimination of ammonium due to thermal out-gassing at 823 K, thus reducing any blocking effect on microporous structures [15].

Results summarised in Table 1 also show that the content of compensating cations of zeolite samples decreases after the chemical treatments applied here. Although the de-cationisation treatment using ion-exchange with ammonium sulphate effectively reduces the amount of compensating cations (Na, K, Mg, Ca); the Si/Al ratio of the zeolite framework does not show a significant change. A considerable amount of calcium and sodium cations migrates to the solution during chemical modification, while magnesium and potassium cations are exchanged at a lower extent. Magnesium and potassium cations seem to be hard to access due to their large radius (e.g. $Mg^{2+}$ has an atomic radius of 0.16 nm; whereas $K^+$, $Ca^{2+}$ and $Na^+$ have an atomic radius of 0.133 nm, 0.104 nm and 0.098 nm, respectively). Sodium ions in natural clinoptilolite zeolites have been reported to be weakly bonded to zeolite lattice and are easy to remove [21]. Moreover, helium pycnometry technique reveals the true density of zeolite samples. The value of true density of NZ decreases from 2.30 to 2.26 g $cm^{-3}$ after acid treatment. In the case of ammonium-exchanged zeolites, density values fall to 2.10 and 2.11 g $cm^{-3}$ for NH4Z1 and 2NH4Z1, respectively.

Acidic properties were determined by Infrared (IR) spectroscopic using pyridine as a probe molecule (99.5% purity supplied by Fluka) in a conventional IR cell of a Nicolet Magna-IR 550 spectrometer, using a pressed disc containing 2 mg of the zeolite sample and 100 mg of KBr, according to experimental procedures reported elsewhere [22]. Samples were previously out-gassed at 623 K or 773 K for 2 h, and then pyridine was introduced into the IR cell at 293 K and maintained for 24 h. After that, non-adsorbed pyridine was removed at 423 K, 523 K, 623 K, 723 K or 773 K (heating temperature) under vacuum. This thermal desorption procedure allows to determine the acidity strength of Lewis and Brønsted

**Table 1**
Physical–chemical characterisation of zeolite samples.

| Sample | $S_{623K}$ ($m^2\ g^{-1}$) | $S_{823K}$ ($m^2\ g^{-1}$) | $SiO_2$[a] | $Al_2O_3$[a] | $Na_2O$[a] | CaO[a] | $K_2O$[a] | MgO[a] | $TiO_2$[a] | $Fe_2O_3$[a] | MnO[a] | Si/Al ratio | $\rho$[b] ($g\ cm^{-3}$) |
|---|---|---|---|---|---|---|---|---|---|---|---|---|---|
| NZ | 205 | 170 | 75.25 | 14.1 | 1.89 | 4.57 | 0.74 | 0.66 | 0.42 | 2.31 | 0.05 | 5.34 | 2.30 |
| ZH2.4 | 434 | 369 | 82.71 | 11.65 | 0.43 | 1.48 | 0.64 | 0.39 | 0.48 | 2.19 | 0.04 | 7.1 | 2.26 |
| NH4Z1 | 181 | 222 | 78.07 | 14.69 | 0.68 | 2.36 | 0.67 | 0.46 | 0.46 | 2.55 | 0.05 | 5.32 | 2.10 |
| 2NH4Z1 | 171 | 261 | 79.26 | 14.85 | 0.26 | 1.82 | 0.39 | 0.37 | 0.47 | 2.53 | 0.05 | 5.34 | 2.11 |

[a] By XRF (% w).
[b] By Helium pycnometry.

acid sites by evaluating the amount of remaining adsorbed pyridine as temperature increases. Lewis and Brønsted acid sites that are detected above 623 K are considered as strong acidic sites [16]. Finally, samples were cooled down to room temperature and IR spectra were collected at an average of 64 scans and a resolution of 2 $cm^{-1}$. Surface concentrations of Brønsted and Lewis acid sites were calculated using the following equation [23]:

$$q_{s\text{-}Py} = \frac{A_p \pi r_{pd}^2}{\xi_m w_{pd}} \times 1000 \quad (1)$$

where $q_{s\text{-}Py}$ represents surface acidic site concentration ($\mu mol\ g^{-1}$); $A_p$ is the integrated absorbance band relative to the adsorbed pyridine ($cm^{-1}$), at Brønsted acid sites (1545 $cm^{-1}$) or at Lewis acid sites (1450 $cm^{-1}$); $r_{pd}$ is the radius of the pressed-disc (cm); $\xi_m$ is the pyridine molar extinction coefficient (1.13 cm $\mu mol^{-1}$ for Brønsted acid sites and 1.28 cm $\mu mol^{-1}$ for Lewis acid sites [24]) and $w_{pd}$ is the mass of the pressed-disc (mg).

Chemical surface characteristics of zeolite samples were identified by FTIR spectroscopy, using a Bruker Mod Tensor 27 apparatus. Spectra from untreated samples and those after sequential adsorption-ozonation experiments were collected at an average 100 scans with a resolution of 4 $cm^{-1}$, using a pressed-disc (1% zeolite in KBr).

### 2.3. Experimental procedures

Toluene adsorption isotherms were performed using static volumetric flasks, as described in a previous study [25]. Sequential adsorption-ozonation experiments were carried out in a fixed-bed flow contactor (45 mm ID), using 50 g of zeolite sample and operating at 293 K and 101 kPa, as described elsewhere [26]. The inlet concentration of toluene ($C_{Tin}$) was fixed by bubbling dry air into pure liquid toluene using a temperature controlled bath (293 K) and diluted to a desired concentration by mixing with a fresh dry air stream. A 4.5 $dm^3\ min^{-1}$ stream containing 22.2 $\mu mol\ dm^{-3}$ toluene was continuously supplied over the zeolite bed until saturation was reached. Then, toluene was replaced by ozone (4.5 $dm^3\ min^{-1}$; 24.3 g $O_3\ dm^{-3}$) and ozone-based oxidative regeneration of toluene-saturated zeolite samples was performed.

### 2.4. Analytical methods

Toluene concentrations at the inlet and outlet streams were monitored on-line by gas chromatography using a VARIAN CP-3800 gas chromatographer equipped with a CP-SIL 8 capillary column (30 m × 0.53 mm ID and a 1.0 μm film thickness) and coupled to a flame ionisation detector operating at 523 K. Separations were conducted under isothermal conditions at 403 K, during 4 min. Ozone concentration was registered on-line, using a BMT 963 ozone analyser.

Adsorbed toluene oxidation by-products were desorbed from regenerated zeolite samples after mixing 1 g of zeolite sample with 3 g of methanol in a closed amber glass flask. Samples were shaken during 48 h and oxidation by-products were detected by High Performance Liquid Chromatography (HPLC) in a Thermo Finning AS 1000 XR apparatus at room temperature (using a mixture of acidify water (pH = 2)/acetonitrile under gradient conditions, a Pronto SIL 120-5-C18 column, and UV-detection at 254 nm).

## 3. Results and discussion

### 3.1. Effect of zeolite chemical surface characteristics on toluene removal

Table 2 lists toluene adsorption isotherm parameters at 293 K on natural and modified zeolite samples after the out-gassing step at 623 K and 823 K. Adsorption equilibrium data are calculated here as the amount of adsorbed toluene per square meter of surface area of zeolite sample ($\mu mol\ m^{-2}$). As it can be seen in Table 2, adsorption isotherms are well represented by the Langmuir adsorption model [27] with a $R^2 > 98\%$, as follows:

$$q = \frac{q_m b C_T}{1 + b C_T} \quad (2)$$

where $q$ is the amount of adsorbed toluene on the zeolite surface at equilibrium ($\mu mol\ m^{-2}$), $C_T$ is the concentration of toluene at equilibrium ($\mu mol\ dm^{-3}$), $q_m$ is the maximum adsorption capacity ($\mu mol\ m^{-2}$), and $b$ is the adsorption intensity or Langmuir coefficient ($dm^3\ \mu mol^{-1}$). The Langmuir sorption model has been widely applied to VOC adsorption on natural and synthetic zeolites [11,12,25,26]. Moreover, the values of separation factors ($R_L$),

**Table 2**
Parameters of Langmuir adsorption model.

| Sample | | $q_m$ ($\mu mol\ m^{-2}$) | $b$ ($dm^3\ \mu mol^{-1}$) | $R^2$ (%) | $R_L$[a] $\times 10^2$ |
|---|---|---|---|---|---|
| NZ | 623 K | 1.46 | 27.35 | 99 | 0.16 |
| ZH2.4 | | 3.27 | 31.67 | 99 | 0.14 |
| NH4Z1 | | 2.07 | 30.06 | 99 | 0.15 |
| 2NH4Z1 | | 5.22 | 9.27 | 98 | 0.48 |
| NZ | 823 K | 0.55 | 108 | 99 | 0.04 |
| ZH2.4 | | 3.07 | 19.77 | 99 | 0.23 |
| NH4Z1 | | 2.76 | 9.02 | 98 | 0.50 |
| 2NH4Z1 | | 3.09 | 19.29 | 99 | 0.23 |

$C_{Tin}$: inlet concentration of toluene.
[a] Separation factor ($R_L$): $R_L = 1/(1 + bC_{Tin})$.

shown in Table 2, are comprised between 0 and 1; indicating the favourability of the adsorption process.

For NZ, ZH2.4 and 2NH4Z1 samples, the maximum adsorption capacity values of the out-gassed samples at 623 K are higher than those values obtained for the out-gassed zeolites at 823 K. However, the value of maximum adsorption capacity registered by the out-gassed NH4Z1 sample at 623 K is slightly lower than the value obtained at 823 K. This lower value in the maximum adsorption capacity could be compensated with a higher value in the adsorption intensity coefficient registered by the out-gassed NH4Z1 sample at 623 K. The lowest adsorption capacity is achieved when natural zeolite is used. On the contrary, the highest adsorption capacity among all samples is reached by the out-gassed 2NH4Z1 sample at 623 K. Under such out-gassing conditions, a high content of Brønsted acid sites is generated on 2NH4Z1 zeolite sample as a consequence of the ammonium exchange treatment followed by thermal modification, as it has been indicated in a previous study [11]. Hence, Brønsted acid sites might be responsible for the observed enhancement on the adsorption capacity of 2NH4Z1 zeolite. The role of acidic surface sites toward the adsorption of VOCs on natural zeolites is analysed in detail elsewhere [11,12].

Experimental results obtained during the ozonation of toluene-saturated zeolite samples are shown in Figs. 1 and 2. On one hand, Fig. 1 indicates the evolution of the residual dimensionless concentration of ozone for samples previously out-gassed at 623 K (Fig. 1A) and out-gassed at 823 K (Fig. 1B). On the other hand, Fig. 2 depicts the variation of reactor bed temperature for samples previously out-gassed at 623 K (Fig. 2A) and out-gassed at 823 K (Fig. 2B).

Residual dimensionless concentration of ozone is calculated as a ratio of the ozone concentration at the outlet stream to the ozone concentration at the inlet stream. Results indicate that higher ozone consumptions, are observed in the out-gassed NH4Z1 and 2NH4Z1 samples at 823 K (see Figs. 1A and B). Indeed, the zeolite sample 2NH4Z1 (out-gassed at 823 K) registers the highest ozone consumption. However, the sample ZH2.4 shows the highest temperature change (about 23 K) when out-gassing thermal pre-treatment at 623 K or 823 K is applied (see Figs. 2A and B). The maximum increase on temperature shown by ZH2.4 sample is registered at around 2000 s, which is related to the total ozone consumption observed up to 3000 s. The increase on zeolite microporosity after the acid treatment could lead to multilayer adsorption of toluene on the ZH2.4 sample. Hence, the observed increase on reactor temperature during the oxidative regeneration of saturated ZH2.4 sample might be as a consequence of ozone reaction with multilayer adsorbed toluene.

After the ozone oxidative regeneration of toluene-saturated zeolites a 28%, 57%, 18% and 17% of the initial adsorption capacity is recovered for NZ, ZH2.4, NH4Z1 and 2NH4Z1 samples (previously out-gassed at 623 K), respectively; whereas the recovery of adsorption capacity for the out-gassed zeolite samples at 823 K are 22%, 57%, 28% and 22% for NZ, ZH2.4, NH4Z1 and 2NH4Z1, respectively. The highest degree of recovery on the adsorption capacity for ZH2.4 sample could be associated to a thermal desorption of oxidation by-products during the ozonation step, as a consequence of the observed increase in the reactor bed temperature. When toluene-saturated 2NH4Z1 sample (out-gassed at 823 K) is regenerated with ozone, the highest ozone consumption is registered. Ozone could not only be consumed by the adsorbed toluene but also by a surface decomposition mechanism that could take place at Lewis acid sites [13].

Results shown in Table 3 reveal the presence of Brønsted and Lewis acid sites with different strength, obtained by IR spectroscopic analysis using pyridine as a probe molecule. As the heating temperature increases from 423 K to 773 K, weak acidic sites disappear and only strong acidic sites are detected. In the case of ammonium exchange zeolites out-gassed at 823 K, the results show an increase on strong Lewis acid sites as the temperature increase. Ammonium ion-exchange treatments followed by thermal out-gassing at 823 K, could reduce pyridine diffusion resistance inside the zeolite framework, leading to an increase on the detection of adsorbed pyridine at stronger Lewis acid sites in such zeolite samples. The concentration of Brønsted acid sites on modified zeolites is higher than on NZ sample. Lewis acid sites increase from NZ to 2NH4Z1. On one hand, the high ozone consumption registered for the sample 2NH4Z1 (out-gassed at 823 K) could be due to its high concentration of strong Lewis acid sites. On the other hand, the high toluene adsorption capacity observed for the sample 2NH4Z1 (out-gassed at 623 K) could be related to its high concentration of strong Brønsted acid sites. Brønsted acid sites could be the main surface sites responsible of toluene adsorption; whereas Lewis acid sites could be mainly related to ozone decomposition and the generation of active oxygen species. During the oxidative regeneration with ozone, surface oxidation reactions could take part among adsorbed toluene at Brønsted acid sites and surface atomic oxygen species generated at Lewis acid sites, reducing the amount of adsorbed toluene on zeolite surface.

**Table 3**
Brønsted and Lewis acidity content of zeolite samples detected by IR at different heating temperatures using pyridine as a probe molecule.

| Sample | Out-gassing temperature | $q_{s\text{-}Py}$ (μmol g$^{-1}$) | | Heating temperature (K) |
|---|---|---|---|---|
| | | Brønsted | Lewis | |
| NZ | 623 K | 32.7 | 76.3 | 423 |
| | | 52.4 | 48.1 | 523 |
| | | 23.5 | 60.0 | 623 |
| | | 0.7 | 44.4 | 723 |
| | | 0.4 | 31.1 | 773 |
| | 773 K | 18.8 | 172.9 | 423 |
| | | 48.8 | 93.3 | 523 |
| | | 26.2 | 91.9 | 623 |
| | | 9.6 | 52.5 | 723 |
| | | 1.4 | 42.8 | 773 |
| ZH2.4 | 623 K | 433.8 | 115.8 | 423 |
| | | 383.9 | 104.4 | 523 |
| | | 297.3 | 76.9 | 623 |
| | | 125.7 | 70.2 | 723 |
| | | 64.6 | 72.0 | 773 |
| | 773 K | 487.6 | 114.2 | 423 |
| | | 490.1 | 84.5 | 523 |
| | | 368.7 | 76.6 | 623 |
| | | 175.2 | 68.8 | 723 |
| | | 92.9 | 70.3 | 773 |
| NH4Z1 | 623 K | 516.6 | 47.8 | 423 |
| | | 514.5 | 43.8 | 523 |
| | | 509.0 | 53.8 | 623 |
| | | 372.6 | 60.0 | 723 |
| | | 281.2 | 60.5 | 773 |
| | 773 K | 263.2 | 48.4 | 423 |
| | | 312.6 | 49.4 | 523 |
| | | 266.9 | 91.3 | 623 |
| | | 243.5 | 139.5 | 723 |
| | | 189.0 | 165.0 | 773 |
| 2NH4Z1 | 623 K | 715.6 | 96.3 | 423 |
| | | 851.2 | 71.9 | 523 |
| | | 723.9 | 69.1 | 623 |
| | | 432.9 | 162.3 | 723 |
| | | 274.5 | 201.9 | 773 |
| | 773 K | 301.4 | 200.3 | 423 |
| | | 312.6 | 194.1 | 523 |
| | | 302.7 | 207.0 | 623 |
| | | 233.1 | 260.5 | 723 |
| | | 179.8 | 282.8 | 773 |

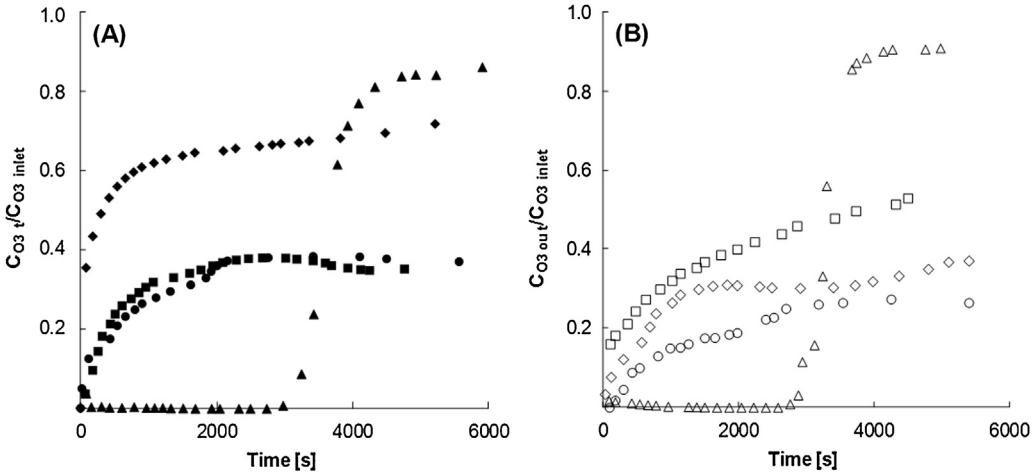


**Fig. 1.** Evolution of residual dimensionless concentration of ozone during ozonation of toluene saturated-zeolites: (A) thermal out-gassed zeolite samples at 623 K; (B) thermal out-gassed zeolite samples at 823 K (■/□) NZ, (▲/△) ZH2.4, (♦/◊) NH4Z1, (●/○) 2NH4Z1. Experimental conditions: 50 g of zeolite, 4.5 $dm^3\ min^{-1}$, 101 kPa, 293 K, $C_{O_3\ inlet} = 23.4\ g\ m^{-3}$.

### 3.2. FTIR study of natural and modified zeolite samples

IR spectra for NZ, ZH2.4, NH4Z1, and 2NH4Z1 zeolite samples upon the out-gassing pre-treatment at 623 K (and at 823 K) without toluene adsorption, after toluene adsorption at 293 K, and after oxidative regeneration using gaseous ozone; are shown in Figs. 3–6, respectively.

As it can be seen in all figures, IR bands around 1100 $cm^{-1}$ and 795 $cm^{-1}$ are observed in all spectra of the zeolite samples prior to toluene adsorption (dotted line). The bands near 1100 $cm^{-1}$ and around 795–800 $cm^{-1}$ are attributed to Si–O vibrations of amorphous silica normally present in the network of natural zeolites and clays [20,28]. These absorption bands are shifted to: 1041 $cm^{-1}$ (NZ-623 K), 1045 $cm^{-1}$ (NZ-823 K), 1082 $cm^{-1}$ (ZH2.4-623 K and ZH2.4-823 K), 1043 $cm^{-1}$ (NH4Z1-623 K), 1057 $cm^{-1}$ (NH4Z1-823 K) and 1047 $cm^{-1}$ (2NH4Z1-623 K and 2NH4Z1-823 K). The highest observed intensity bands at 1082 $cm^{-1}$ and 795 $cm^{-1}$ are recorded by ZH2.4 sample. These results are in agreement with those obtained by XRF analyses, showing the biggest silica content of this zeolite sample (see Table 1). Additionally, the absorption band around 1630 $cm^{-1}$ is observed in all samples; which has been assigned to the deformation band of adsorbed water [12]. Stretching vibrations at around 3625 $cm^{-1}$ and 3440 $cm^{-1}$ could be associated to coordinated water on zeolite surface [29]

Recorded IR spectrum after toluene adsorption (dashed line) on NZ sample (out-gassed at 623 K and 823 K), registers a band at 1420 $cm^{-1}$, assigned to C=C stretching vibration corresponding to the aromatic ring of toluene molecule. This band is slightly shifted to a lower frequency, compared to the C=C stretching vibration of toluene in the gaseous phase (see Figs. 3A and B). Similarly, a band at 1520 $cm^{-1}$ is registered for ZH2.4 zeolites (see Figs. 4A and B). IR spectra of ammonium-exchanged zeolite samples, NH4Z1 (see Figs. 5A and B) and 2NH4Z1 (see Figs. 6A and B) out-gassed at 623 K and 823 K show a band at 1470 $cm^{-1}$ after toluene adsorption. An absorption band in the region around 1450–1540 $cm^{-1}$ with a maximum at 1477 $cm^{-1}$ has been associated to adsorbed toluene on zeolites [30]. Such experimental results confirm that toluene is chemically adsorbed on zeolite surface. For the out-gassed NH4Z1 samples at 623 K and 823 K an increase on the intensity of an absorption band at 1470 $cm^{-1}$ could be associated to the C=C aromatic ring stretching mode of toluene molecule. This absorption band is shifted to a lower wavenumber compared to that of gaseous toluene at 1506 $cm^{-1}$. This band displacement could be attributed to changes in electronic distribution and the symmetry of the aromatic ring when it interacts with the zeolite structure [29]. Similar

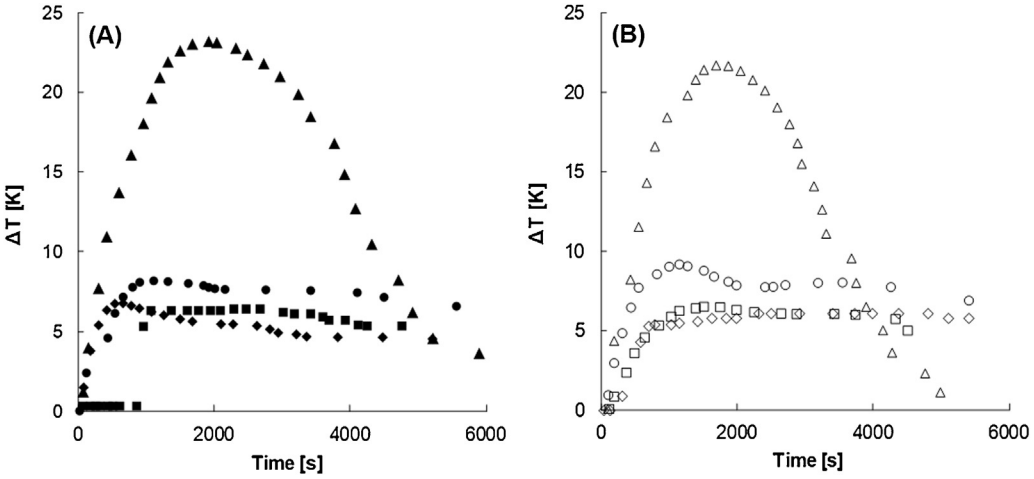


**Fig. 2.** Variation on the reactor bed temperature during ozonation of toluene saturated-zeolites: (A) thermal out-gassed zeolite samples at 623 K; (B) thermal out-gassed zeolite samples at 823 K. (■/□) NZ, (▲/△) ZH2.4, (♦/◊) NH4Z1, (●/○) 2NH4Z1. Experimental conditions: 50 g of zeolite, 4.5 $dm^3\ min^{-1}$, 101 kPa, 293 K, $C_{O_3\ inlet} = 23.4\ g\ m^{-3}$.

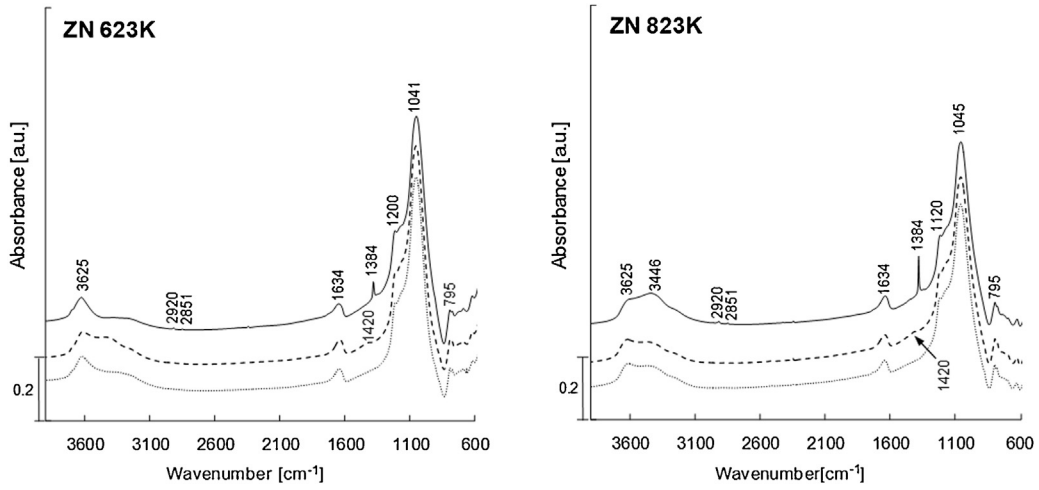


**Fig. 3.** FTIR spectra of natural zeolite (NZ): (A) out-gassed at 623 K; (B) out-gassed at 823 K. Dotted line represents NZ sample after thermal treatment, dashed line represents toluene saturated-NZ sample, and solid line represents regenerated NZ after ozonation.

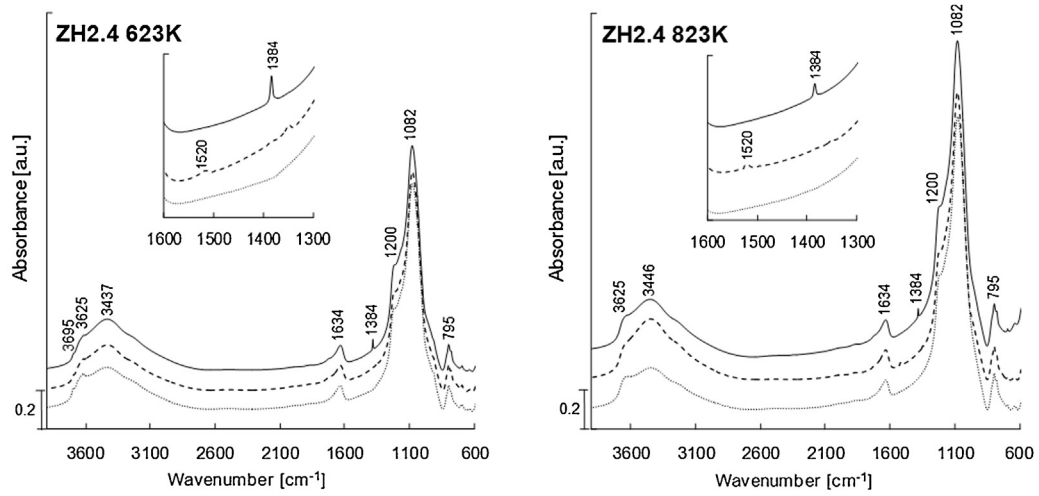


**Fig. 4.** FTIR spectra of acid-modified natural zeolite (ZH2.4): (A) out-gassed at 623 K; (B) out-gassed at 823 K. Dotted line represents ZH2.4 sample after thermal treatment, dashed line represents toluene saturated-ZH2.4 sample, and solid line represents regenerated ZH2.4 sample after ozonation.

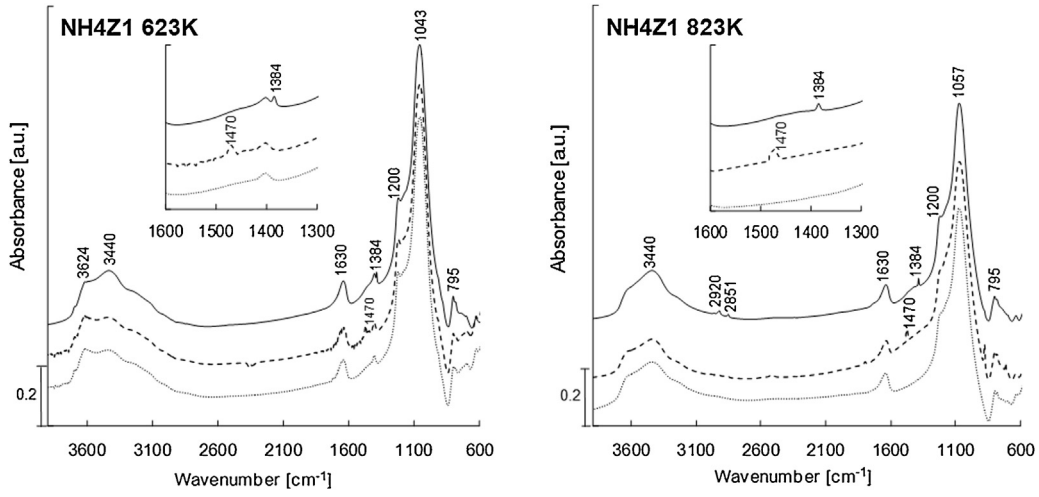


**Fig. 5.** FTIR spectra of ammonium-modified natural zeolite (NH4Z1): (A) out-gassed at 623 K; (B) out-gassed at 823 K. Dotted line represents NH4Z1 sample after thermal treatment, dashed line represents toluene saturated-NH4Z1 sample, and solid line represents regenerated NH4Z1 sample after ozonation.

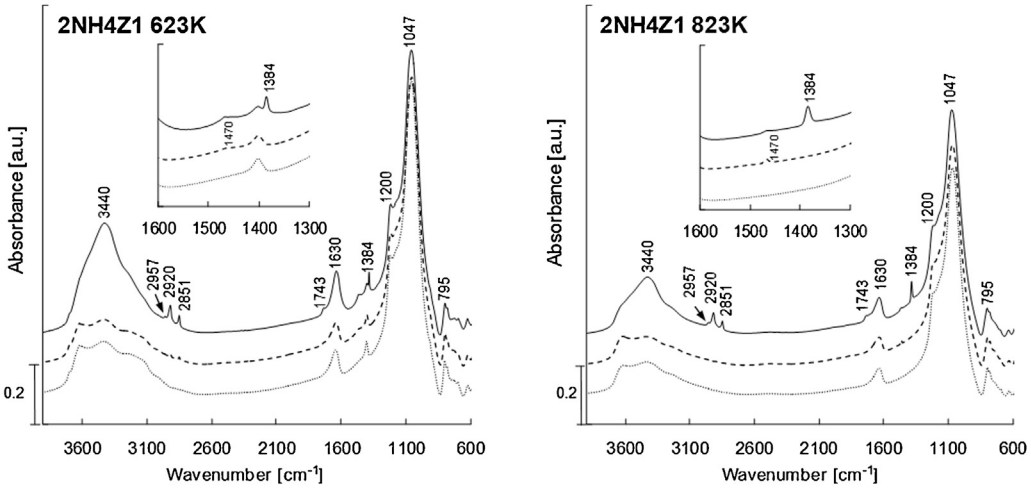


**Fig. 6.** FTIR spectra of twice ammonium-modified natural zeolite (2NH4Z1): (A) out-gassed at 623 K; (B) out-gassed at 823 K. Dotted line represents 2NH4Z1 sample after thermal treatment, dashed line represents toluene saturated-2NH4Z1 sample, and solid line represents regenerated 2NH4Z1 sample after ozonation.

trend is observed in the case of benzene interacting with the OH group of zeolites [31]. Hence, results obtained here could be related to toluene interaction with a higher content of Brønsted acid sites, as shown Table 3.

Additionally, an IR absorption band around 1420 $cm^{-1}$ is observed for the out-gassed ammonium-exchanged zeolite samples at 623 K, NH4Z1 (see Fig. 5A) and 2NH4Z1 (see Fig. 6A), prior to the adsorption of toluene. This absorption band can still be seen in these samples after toluene adsorption and even after the oxidative regeneration with ozone. However, this band does not appear in the spectra of the out-gassed ammonium-exchanged zeolite samples at 823 K, NH4Z1 (see Fig. 5B) and 2NH4Z1 (see Fig. 6B). Such behaviour could be related to some ammonium molecules ($NH_4^+$) that remain adsorbed on the out-gassed samples at 623 K and are finally desorbed after the thermal out-gassing pre-treatment at 823 K. These results are in agreement with those reported by another research group who associates an IR band around 1430 $cm^{-1}$ to adsorbed ammonium on zeolite samples [32].

As it can be appreciated in all figures, the IR spectra after oxidative regeneration with ozone (solid line) show a common absorption band at 1384 $cm^{-1}$ for all out-gassed zeolite samples. This IR band could be related to active oxygen surface species generated after ozone decomposition on acidic sites. Several studies have assigned the IR absorption band at 1380 $cm^{-1}$ to active atomic oxygen on zeolites surface, generated after ozone decomposition at Lewis acid surface sites [33–39]. Previous studies have suggested the interaction of surface atomic oxygen with organic compounds such as toluene [6,40]. Moreover, an increase on the intensity of the absorption band observed at 1384 $cm^{-1}$, could be associated to a higher content of Lewis acid sites present on the out-gassed samples at 823 K in comparison to the out-gassed samples at 623 K, as shown in Table 3. The density of Lewis acid sites is increased after the out-gassing treatment at 823 K due to that Brønsted acid sites are converted into new Lewis acid sites. Hence, a high content of Lewis acid sites are available for ozone adsorption and transformation into active oxygen species.

Two distinctive bands can be seen at 2851 and 2920 $cm^{-1}$, after ozone regenerative oxidation of adsorbed toluene (solid line) on NZ out-gassed at 623 K and 823 K (see Figs. 3A and B), NH4Z1 out-gassed at 823 K (see Fig. 5B), and 2NH4Z1 out-gassed at 623 K and 823 K (see Figs. 6A and B). A band at 2957 $cm^{-1}$ is observed in 2NH4Z1 samples (out-gassed at 623 K and 823 K). Bands at 2899 and 2935 $cm^{-1}$ have been related to the (C–H) stretching vibrations of formate species [41]. In this study, such IR absorption bands could be shifted to 2851, 2920 and 2957 $cm^{-1}$ and might be an evidence of the formation of toluene oxidation by-products that remain adsorbed on zeolite surface after ozone regeneration treatment. These IR bands are not registered in the spectra of regenerated ZH2.4 samples; showing that less oxidation by-products remain adsorbed [41]. However, a high amount of toluene remains adsorbed on ZH2.4 sample (out-gassed at 623 K and 823 K) after ozone regeneration, as indicated by HPLC analyses. Such experimental results could be associated to a lower activity of Lewis acid sites of this sample. A similar trend is observed for NH4Z1 out-gassed at 623 K, as consequence of its lower content of Lewis acid sites. Aditionally, a band at 1743 $cm^{-1}$ is observed in the collected spectra for the ozonation of toluene saturated-2NH4Z1 samples. In another publication, the band around 1752 $cm^{-1}$ has been associated to formic acid [42].

HPLC technique allows identifying a narrow band of oxidation by-products that remain adsorbed on zeolite surface after the oxidative regeneration with ozone. As a consequence of ozone-toluene surface reactions; formic acid, acetaldehyde, benzoic acid, benzaldehyde are detected here, as the main intermediate compounds of toluene oxidation. The highest concentration level of formic acid is detected for NZ sample out-gassed at 623 K. Similarly, high concentrations of acetaldehyde, benzaldehyde and benzoic acid are registered in ZH2.4 (out-gassed at 623 K), NZ (out-gassed at 823 K) and NZ (out-gassed at 623 K) samples, respectively. The high concentration levels of formic acid, benzoic acid and benzaldehyde observed in NZ sample (out-gassed at 623 K), could be related to a lower catalytic activity toward ozone, as it has been previously suggested [14].

Moreover, the concentration of toluene that remains adsorbed inside zeolite channels after oxidative regeneration with ozone, decreases in the following order: ZH2.4-623 K > ZH2.4-823 K > NZ-623 K > NH4Z1-823 K > NZ-823 K > NH4Z1-623 K > 2NH4Z1-823 K > 2NH4Z1-623 K. The presence of adsorbed toluene after the ozone regeneration process applied here could be related to a combination of factors, which involve a high adsorption capacity of toluene and a low catalytic activity toward ozone of some zeolite samples. Thus, the highest registered concentration of toluene for ZH2.4 sample (out-gassed at 623 K) could correspond to a high toluene adsorptive capacity and a lower catalytic activity toward ozone, as reported elsewhere [11,14]. Acetaldehyde and benzaldehyde have been identified as oxidation by-products of toluene reaction with ozone in the presence of synthetic zeolites [6]. In addition, formic and benzoic acids have already been reported as

the main intermediates of toluene reaction with ozone [43]. These results are in agreement with those obtained by FTIR analyses where IR bands registered at around 2851–2920 $cm^{-1}$ and at 1743 $cm^{-1}$ are associated to adsorbed oxidation by-products, such as formic acid, acetaldehyde, benzoic acid and benzaldehyde (see Figs. 3A, B, 5B, 6A and B). As discussed before, these oxidation by-products might be responsible for the observed reduction in toluene adsorption capacity after ozone oxidative-regeneration of toluene saturated-zeolite samples.

Results obtained here suggest that a surface reaction mechanism could take place among toluene molecules adsorbed at Brønsted acid sites and surface active oxygen species generated after ozone decomposition at Lewis acid sites. As a consequence of such surface interactions, intermediate products such as formic acid, acetaldehyde, benzoic acid and benzaldehyde are generated. These findings are in agreement with other published research studies [44,45].

## 4. Conclusions

Experimental results obtained here show that single ozone gas regeneration would not be suitable to regenerate the adsorption capacity of toluene-saturated natural zeolites. Indeed, the presence of adsorbed toluene oxidation by-products on the zeolite surface impairs the regeneration process. The highest degree of recovery on the adsorption capacity is obtained when acid-treated zeolite is used (ZH2.4), probably due to the desorption of adsorbed species as a consequence of temperature increase during the regeneration step. Moreover, results indicate that acidic surface sites in the form of Brønsted acid sites could be responsible for toluene adsorption, whereas Lewis acid sites could be mainly associated to ozone decomposition and the generation of surface active oxygen species. Toluene molecules adsorbed at Brønsted acid sites seem to react with surface active oxygen species generated by ozone gaseous decomposition at Lewis acid sites. A sequential adsorption-ozonation followed by thermal regeneration could be an attractive option for VOCs removal.

## Acknowledgements

The authors wish to thank CONICYT, FONDECYT/Regular (Grant No. 1130560), ANR (Grant No. ANR-10-ECOT-011-01), ECOS/CONICYT Program (Grant No. C11E08), and BASAL PFB-27 for their financial support. S. Alejandro expresses his gratitude to the France Embassy in *Santiago de Chile* for providing a mobility doctoral scholarship and to Dr. N. Brodu from *Université de Toulouse, INPT, UPS, Laboratoire de Génie Chimique* for his valuable collaboration. H. Valdés gratefully acknowledges funding under *CNRS Délégation Midi-Pyrénées* contract 424948.

## References

[1] B. Lu, X. Zhang, X. Yu, T. Feng, S. Yao, Catalytic oxidation of benzene using DBD corona discharges, J. Hazard. Mater. 137 (2006) 633–637.
[2] J. Pires, A. Carvalho, M.B. de Carvalho, Adsorption of volatile organic compounds in Y zeolites and pillared clays, Micropor. Mesopor. Mat. 43 (2001) 277–287.
[3] F.I. Khan, A.K. Ghoshal, Removal of volatile organic compounds from polluted air, J. Loss Prevent. Proc. 13 (2000) 527–545.
[4] A.K. Ghoshal, S.D. Manjare, Selection of appropriate adsorption technique for recovery of VOCs: an analysis, J. Loss Prevent. Proc. 15 (2002) 413–421.
[5] S. Ojala, S. Pitkäaho, T. Laitinen, N.N. Koivikko, R. Brahmi, J. Gaálová, A.K. Lenka Matejova, Sanna Päivärinta, Christian Hirschmann, T. Nevanperä, M. Riihimäki, M. Pirilä, R.L. Keiski, Catalysis in VOC abatement, Top. Catal. 54 (2011) 1224–1256.
[6] C.Y.H. Chao, C.W. Kwong, K.S. Hui, Potential use of a combined ozone and zeolite system for gaseous toluene elimination, J. Hazard. Mater. 143 (2007) 118–127.
[7] H. Einaga, Y. Teraoka, A. Ogat, Benzene oxidation with ozone over manganese oxide supported on zeolite catalysts, Catal. Today 164 (2011) 571–574.
[8] P. Monneyron, S. Mathé, M.H. Manero, J.N. Foussard, Regeneration of high silica zeolites via advanced oxidation processes—a preliminary study about adsorbent reactivity toward ozone, Chem. Eng. Res. Des. 81 (2003) 1193–1198.
[9] P. Monneyron, M.H. Manero, S. Manero, A combined selective adsorption and ozonation process for VOCs removal from air, Can. J. Chem. Eng. 85 (2007) 326–332.
[10] N. Brodu, H. Zaitan, M.-H. Manero, J.-S. Pic, Removal of volatile organic compounds by heterogeneous ozonation on microporous synthetic alumino silicate, Water Sci. Technol. 66 (2012) 2020–2026.
[11] S. Alejandro, H. Valdés, M.H. Manero, C.A. Zaror, BTX abatement using Chilean natural zeolite: the role of Bronsted acid sites, Water Sci. Technol. 66 (2012) 1759–1769.
[12] H. Valdés, V. Solar, E.H. Cabrera, A.F. Veloso, C.A. Zaror, Control of released volatile organic compounds from industrial facilities using natural and acid-treated mordenites: the role of acidic surface sites on the adsorption mechanism, Chem. Eng. J. 244 (2014) 117–127.
[13] H. Valdés, E. Padilla, C.A. Zaror, Influence of chemical surface characteristics of natural zeolite on catalytic ozone abatement, Ozone-Sci. Eng. 33 (2011) 279–284.
[14] S. Alejandro, H. Valdés, C.A. Zaror, Natural zeolite reactivity towards ozone: the role of acid surface sites, J. Adv. Oxid. Technol. 14 (2011) 182–189.
[15] H. Valdés, S. Alejandro, C.A. Zaror, Natural zeolite reactivity towards ozone: the role of compensating cations, Chem. Eng. J. 227–228 (2012) 34–40.
[16] N. Brodu, M.-H. Manero, C. Andriantsiferana, J.-S. Pic, H. Valdés, Role of Lewis acid sites of ZSM-5 zeolite on gaseous ozone abatement, Chem. Eng. J. 231 (2013) 281–286.
[17] T.-T. Win-Shwe, H. Fujimaki, Neurotoxicity of toluene, Toxicol. Lett. 198 (2010) 93–99.
[18] H. Valdés, V.J. Farfán, J.A. Manoli, C.A. Zaror, Catalytic ozone aqueous decomposition promoted by natural zeolite and volcanic sand, J. Hazard. Mater. 165 (2009) 915–922.
[19] M. Viana, P. Jouannin, C. Pontier, D. Chulia, About pycnometric density measurements, Talanta 57 (2002) 583–593.
[20] A. Ates, C. Hardacre, The effect of various treatment conditions on natural zeolites: ion exchange, acidic, thermal and steam treatments, J. Colloid Interface Sci. 372 (2012) 130–140.
[21] S.J. Allen, E. Ivanova, B. Koumanova, Adsorption of sulfur dioxide on chemically modified natural clinoptilolite. Acid modification, Chem. Eng. J. 152 (2009) 389–395.
[22] A. Simon-Masseron, J.P. Marques, J.M. Lopes, F.R.a. Ribeiro, I. Gener, M. Guisnet, Influence of the Si/Al ratio and crystal size on the acidity and activity of HBEA zeolites, App. Catal. A-Gen. 316 (2007) 75–82.
[23] C.A. Emeis, Determination of integrated molar extinction coefficients for infrared absorption bands of pyridine adsorbed on solid acid catalysts, J. Catal. 141 (1993) 347–354.
[24] K.L. Konan, C. Peyratout, A. Smith, J.P. Bonnet, P. Magnoux, P. Ayrault, Surface modifications of illite in concentrated lime solutions investigated by pyridine adsorption, J. Colloid Interface Sci. 382 (2012) 17–21.
[25] S. Brosillon, M.H. Manero, J.N. Foussard, Mass transfer in VOC adsorption on zeolite: experimental and theoretical breakthrough curves, Environ. Sci. Technol. 35 (2001) 3571–3575.
[26] P. Monneyron, M.H. Manero, J.N. Foussard, Measurement and modeling of single- and multi-component adsorption equilibria of VOC on high-silica zeolites, Environ. Sci. Technol. 37 (2003) 2410–2414.
[27] I. Langmuir, The constitution and fundamental properties of solids and liquids. Part I. Solids, J. Am. Chem. Soc. 38 (1916) 2221–2295.
[28] J. Madejová, FTIR techniques in clay mineral studies, Vib. Spectrosc. 31 (2003) 1–10.
[29] R.M. Serra, E.E. Miró, A.V. Boix, FTIR study of toluene adsorption on Cs-exchanged mordenites, Micropor. Mesopor. Mat. 127 (2010) 182–189.
[30] R.R. Malherbe, R. Wendelbo, Study of Fourier transform infrared-temperature-programmed desorption of benzene, toluene and ethylbenzene from H-ZSM-5 and H-beta zeolites, Thermochim. Acta 400 (2003) 165–173.
[31] B.-L. Su, V. Norberg, Quantitative characterisation of H-Mordenite zeolite structure by infrared spectroscopy using benzene adsorption, Colloid Surf. A 187–188 (2001) 311–318.
[32] M. Niwa, K. Suzuki, N. Katada, T. Kanougi, T. Atoguchi, Ammonia IRMS-TPD study on the distribution of acid sites in mordenite, Micropor. Mesopor. Mat. 109 (2005) 18749–18757.
[33] H. Einaga, S. Futamura, Catalytic oxidation of benzene with ozone over alumina-supported manganese oxides, J. Catal. 227 (2004) 304–312.
[34] H. Einaga, A. Ogata, Benzene oxidation with ozone over supported manganese oxide catalysts: effect of catalyst support and reaction conditions, J. Hazard. Mater. 164 (2009) 1236–1241.
[35] B. Kasprzyk-Hordern, M. Ziólek, J. Nawrocki, Catalytic ozonation and methods of enhancing molecular ozone reactions in water treatment, Appl. Catal. B-Environ. 46 (2003) 639–669.
[36] B. Dhandapani, S.T. Oyama, Gas phase ozone decomposition catalysts, Appl. Catal. B-Environ. 11 (1997) 129–166.
[37] K.M. Bulanin, J.C. Lavalley, A.A. Tsyganenko, IR spectra of adsorbed ozone, Colloid Surf. A 101 (1995) 153–158.
[38] K.M. Bulanin, J.C. Lavalley, A.A. Tsyganenko, Infrared study of ozone adsorption on CaO, J. Phys. Chem. B 101 (1997) 2917–2922.
[39] W. Li, S.T. Oyama, Mechanism of ozone decomposition on a manganese oxide catalyst. 2. Steady-state and transient kinetic studies, J. Am. Chem. Soc. 120 (1998) 9047–9052.

[40] H. Einaga, S. Futamura, Catalytic oxidation of benzene with ozone over Mn ion-exchanged zeolites, Catal. Commun. 8 (2007) 557–560.
[41] X.-M. Chen, X.-F. Yang, A.-M. Zhu, H.-Y. Fan, X.-K. Wang, Q. Xin, X.-R. Zhou, C. Shi, In situ DRIFTS study on the partial oxidation of ethylene over Co-ZSM-5 catalyst, Catal. Commun. 10 (2009) 428–432.
[42] J.Y. Jeon, H.Y. Kim, S.I. Woo, Mechanistic study on the SCR of NO by C3H6 over Pt/V/MCM-41, Appl. Catal. B-Environ. 44 (2003) 301–310.
[43] M. Franco, I. Chairez, T. Poznyak, A. Poznyak, BTEX decomposition by ozone in gaseous phase, J. Environ. Manage. 95 (2012) S55–S60.
[44] J. Van Durme, J. Dewulf, W. Sysmans, C. Leys, H. Van Langenhove, Abatement and degradation pathways of toluene in indoor air by positive corona discharge, Chemosphere 68 (2007) 1821–1829.
[45] H. Huang, W. Li, Destruction of toluene by ozone-enhanced photocatalysis: performance and mechanism, Appl. Catal. B-Environ. 102 (2011) 449–453.